# EXIT chart evaluation of a receiver structure for multi-user multi-antenna OFDM systems

Hammarberg, Peter; Rusek, Fredrik; Salvo Rossi, Pierluigi; Edfors, Ove

*Published in:*
Proc. IEEE Global Telecommunications Conference (GLOBECOM) 2009

*DOI:*
10.1109/GLOCOM.2009.5426288

2009

# EXIT Chart Evaluation of a Receiver Structure for Multi-User Multi-Antenna OFDM Systems

Peter Hammarberg*, Fredrik Rusek*, Pierluigi Salvo Rossi† and Ove Edfors*
*Department of Electrical and Information Technology, Lund University, Lund, Sweden.
†Department of Information Engineering, Second University of Naples, Aversa (CE), Italy.

***Abstract*— In this paper we evaluate, by means of Extrinsic Information Transfer (EXIT) charts, an iterative receiver that has emerged as a promising candidate for non-coherent multi-user multi-antenna OFDM systems. The receiver performs parallel interference cancellation (followed by linear filtering) and channel estimation, using soft symbols obtained from a bank of single-user decoders. For the sake of conceptual clarity we study a system with two single antenna users and a receiver with two antennas, and we demonstrate how the convergence behavior of the receiver can be visualized using paired three dimensional EXIT surfaces. Our results show that the actual decoder trajectories obtained through simulations are well predicted from the EXIT charts.**

**For the iterative receiver under investigation we identify a very specific problem with EXIT chart generation; the EXIT curve for the inner component decoder depends on the outer encoder. To handle this problem we propose a modification to the iterative receiver which solves the aforementioned problem; the performance degradation is demonstrated to be small.**

## I. Introduction

In the last few years we have seen a large growth in data traffic over wireless networks. With increasing traffic, capacity of wireless networks must scale proportionally. Future systems thus need to make better use of the available, limited, spectrum and/or search for available resources elsewhere. A number of technologies that provide increased spectral efficiency have been proposed; in particular, multi-antenna systems have received much attention lately. With the use of multi-antenna systems large gains can be harvested due to multiplexing in the spatial domain alongside the frequency and time domains. Multiple antennas at the receiver can also be used to perform multi-user detection (MUD) or interference cancellation, allowing improved resource utilization.

In order to harvest the promised gains, some form of advanced coding method must be used in conjunction with the multi-antenna system. The invention of turbo codes made it possible to implement capacity achieving codes with a reasonable decoding complexity. The convergence behavior of turbo codes can be visualized by the use of EXtrinsic Information Transfer (EXIT) charts, as proposed in [1]. These charts visualize the exchange of mutual information between concatenated code blocks and have become a valuable tool for designing turbo codes.

Since the invention of turbo codes, the turbo principle has successfully been applied to channel equalization [2] and estimation [3] [4], further improving performance of wireless receivers. Also for these applications, EXIT charts have shown to be a helpful tool for visualizing convergence behavior and aid performance evaluation. In, e.g., [5] the convergence behavior of an iterative MIMO receiver is evaluated using EXIT charts, assuming perfect channel state information (PCSI) and a single code stream multiplexed over the antennas. Kansanen [6] treats the case with multiple code streams and shows paired three dimensional (3D) EXIT surfaces for a turbo equalizer, again assuming PCSI. Sand et al. [7] evaluate a receiver with iterative channel estimation and equalization, analyzing the convergence behavior. In [8] a 3D EXIT chart is used to show the information flow between the code, equalizer and channel estimator for a single antenna link.

In this paper we evaluate an iterative receiver, as proposed in [9], by means of EXIT charts. The receiver is intended for multi-user multi-antenna OFDM systems performing parallel interference cancellation and channel estimation, using soft symbols obtained from a block of single user decoders. That is, unlike in above cited work, we look at a system with imperfect channel state information, and multiple code streams. We show how the convergence behavior of the receiver can be visualized using EXIT surfaces. The case of two single antenna users, and a receiver with two antennas, is treated. For this system we show that the corresponding EXIT chart can be visualized using paired 3D charts, one for each user code stream. We also propose changes to the receiver simplifying EXIT chart generation, and look at the convergence region, represented as projections onto a plane. Our results show that the convergence trajectory obtained through simulations are close to the one obtained by the EXIT chart.

The outline of the paper is as follows; in section II the system model and the receiver structure is briefly introduced, followed by a presentation of the EXIT chart representation in section III. Our results are presented in section IV before we conclude our findings in section V.

## II. System Model

A multi-user OFDM system with $K$ users equipped with a single antenna each, and a receiver with $N$ antennas is considered. The users are assumed non-cooperative, i.e. they transmit independent data, but for simplicity we assume them to be synchronous. For the sake of clarity we restrict the presentation to the case $K = N = 2$ with the remark that the extension to arbitrary $N$ and $K$ is straightforward.

This work has been supported by the Swedish Governmental Agency for Innovation Systems (VINNOVA) and by the Research Council of Norway (NFR) under the project WILATI+ within the NORDITE framework.

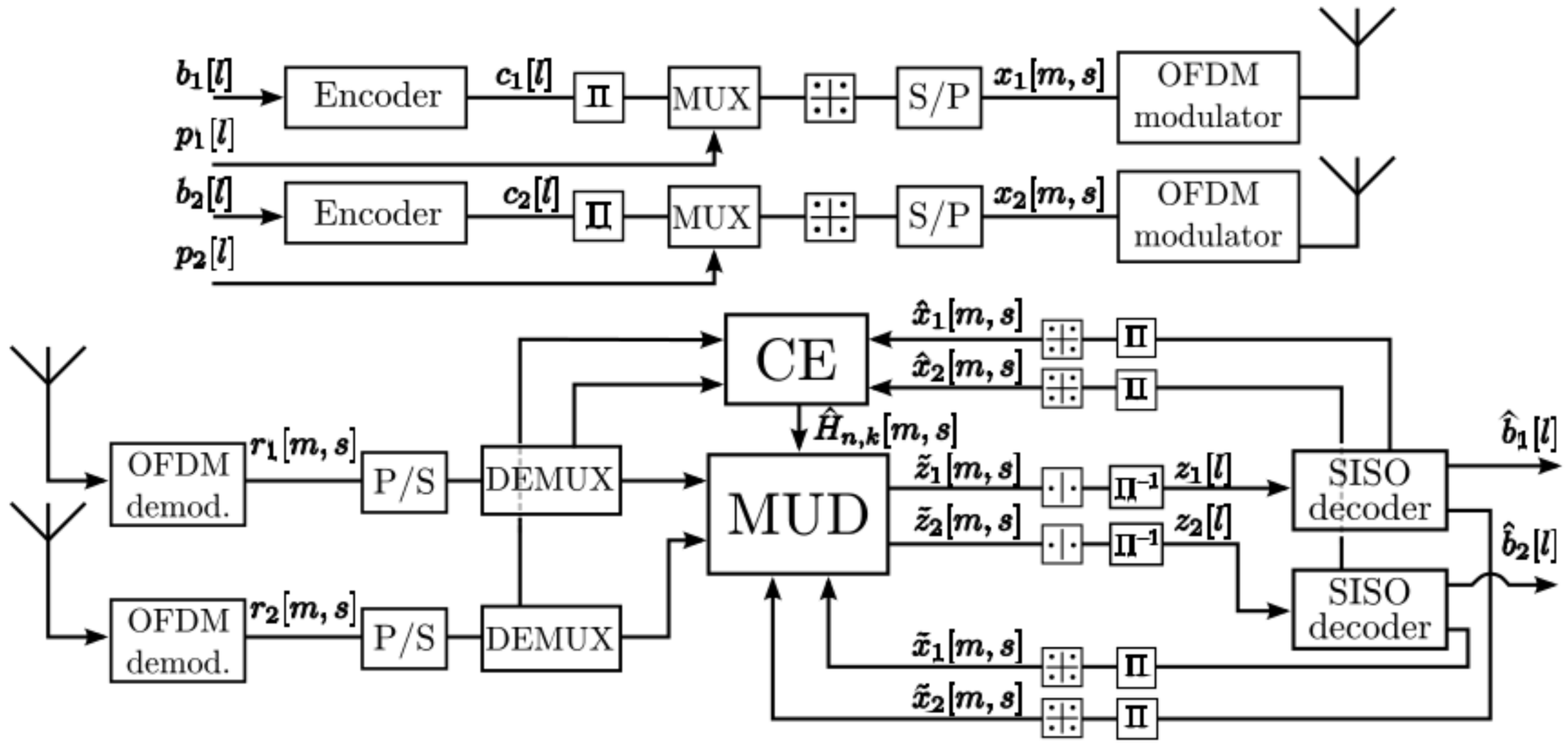


Fig. 1. The structure of the iterative receiver.

The transmit/receive chain is depicted in Fig. 1 for the case considered. Each stream is encoded via convolutional coding and interleaved using an s-random interleaver [10]. QPSK mapping, serial to parallel conversion, and OFDM modulation follows. To provide the iterative receiver with an initial channel estimate, $S_p$ pilot OFDM symbols are inserted. We assume (small) finite packet transmission, with $S$ denoting the total number of OFDM symbols sent from the transmitter within a frame (not to confuse with the interleaver s-parameter); the number of information carrying symbols is thus $S - S_p$. Consequently, each user transmits $2(S-S_p)MR_c$ information bits, where $M$ is the number of subcarriers, $R_c$ is the rate of the encoder and the factor 2 stems from the QPSK modulation. The frame structure is shown in Fig. 2.

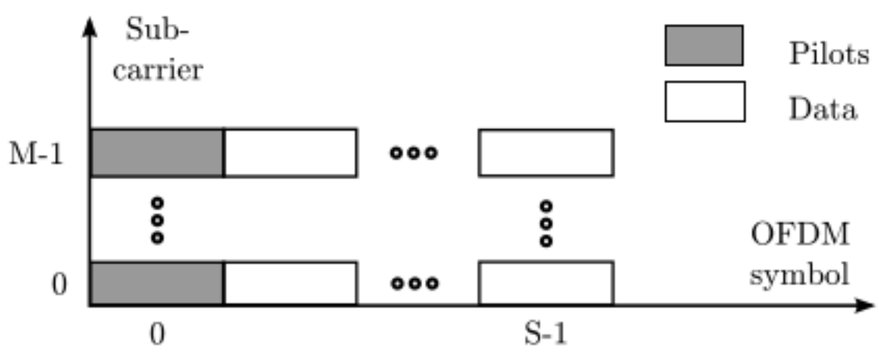


Fig. 2. $M$ subcarrier OFDM frame structure with, in this case, one pilot symbols followed by S-1 data symbols.

Referring to the $m$th subcarrier during transmission of the $s$th OFDM symbol, we denote the transmitted vector, the channel matrix, the AWGN vector ($\sim \mathcal{CN}(\mathbf{0}, \sigma_w^2 \boldsymbol{I})$), and the received vector as

$$\begin{aligned}
\boldsymbol{x}[m,s] &= (x_1[m,s], \ldots, x_K[m,s])^{\mathrm{T}} , \\
\boldsymbol{H}[m,s] &= \begin{pmatrix} H_{1,1}[m,s] & \ldots & H_{1,K}[m,s] \\ \vdots & \ddots & \vdots \\ H_{N,1}[m,s] & \ldots & H_{N,K}[m,s] \end{pmatrix} , \\
\boldsymbol{w}[m,s] &= (w_1[m,s], \ldots, w_N[m,s])^{\mathrm{T}} , \text{and} \\
\boldsymbol{r}[m,s] &= (r_1[m,s], \ldots, r_N[m,s])^{\mathrm{T}} .
\end{aligned}$$

The discrete-time model for the received signal can then be written as

$$\boldsymbol{r}[m,s] = \boldsymbol{H}[m,s]\boldsymbol{x}[m,s] + \boldsymbol{w}[m,s] . \quad (1)$$

Note that $\boldsymbol{H}$ is the multi-user channel, containing the coefficients for all users.

At the receiver, as illustrated in Fig. 1, OFDM symbols are demodulated and sent to the iterative decoder, performing MUD, Soft-Input Soft-Output (SISO) decoding and channel estimation (CE). The multi-user detector and SISO decoders exchange extrinsic information on symbols $x_k$, denoted $\tilde{x}_k$ (resp. $\tilde{z}_k$) when going to the multi-user detector (resp. the SISO decoders). The SISO decoders also provide *a posteriori* information of the transmitted symbols $x_k$, denoted $\hat{x}_k$, to the channel estimator, and *a posteriori* information on source bits. The channel estimator provides channel coefficient estimates ($\hat{H}_{n,k}$).

### A. MUD

Multi-user detection is a demanding task and a number of strategies can be applied. When there is a large number of users $K$ and/or the modulation order grows beyond QPSK, optimum MUD (BCJR-type) is not a viable approach due to its enormous complexity. Therefore, reduced complexity MUDs should be looked into; these can roughly be categorized into linear and non-linear methods. In this paper we adopt a linear approach: Soft interference cancellation + linear MMSE filtering. The associated computational complexity scales linearly with $K$ and is independent of the modulation order. The MUD under investigation was first proposed in [3] for CDMA systems, and adapted to MIMO-OFDM systems in [11].

The received signals (1) are processed separately for each subcarrier and OFDM symbol. Parallel interference cancellation is performed using $\tilde{x}$ from the SISO decoders and $\hat{\boldsymbol{H}}$ from the channel estimators. The residual term from the interference cancellation for the $k$th transmit antennas, $\tilde{\boldsymbol{r}}^{(k)} =$

$\boldsymbol{r} - \hat{\boldsymbol{H}}(\tilde{\boldsymbol{x}} - \tilde{x}_k \boldsymbol{i}_K^{(k)})$, with $\boldsymbol{i}_K^{(k)}$ being the $k$:th column of the $K \times K$ identity matrix $\boldsymbol{I}_K$, is then MMSE filtered to reduce multi-user interference, giving the soft output symbols

$$\tilde{z}_k = \frac{\boldsymbol{i}_K^{(k)\mathrm{T}} \left( \hat{\boldsymbol{H}}^{\mathrm{H}} \hat{\boldsymbol{H}} + \sigma_w^2 (\boldsymbol{V}^{(k)})^{-1} \right)^{-1} \hat{\boldsymbol{H}}^{\mathrm{H}} \tilde{\boldsymbol{r}}^{(k)}}{\boldsymbol{i}_K^{(k)\mathrm{T}} \left( \hat{\boldsymbol{H}}^{\mathrm{H}} \hat{\boldsymbol{H}} + \sigma_w^2 (\boldsymbol{V}^{(k)})^{-1} \right)^{-1} \hat{\boldsymbol{H}}^{\mathrm{H}} \hat{\boldsymbol{h}}_k^{(\mathrm{tx})}}, \quad (2)$$

with $\boldsymbol{V}^{(k)} = \mathrm{diag}\left( (1 - |\tilde{x}_1|^2, \ldots, 1 - |\tilde{x}_{k-1}|^2, 1, 1 - |\tilde{x}_{k+1}|^2, \ldots, 1 - |\tilde{x}_K|^2) \right)$ and $\boldsymbol{h}_k^{(\mathrm{tx})}[m, s]$ denoting the channel vector from the $k$th user. For the derivation we refer to [3].

### B. SISO Decoding

The demapped and deinterleaved output of the MUD is *assumed* to be described by the equation

$$z_k[l] = x_k[l] + v_k[l], \quad k = 1..K, \quad (3)$$

where $v_k[l] \sim \mathcal{N}(0, \eta_k^2)$ with the variance estimated as

$$\eta_k^2 = \frac{1}{\boldsymbol{i}_K^{(k)\mathrm{T}} \left( \boldsymbol{H}^{\mathrm{H}} \boldsymbol{H} + \sigma_w^2 (\boldsymbol{V}^{(k)})^{-1} \right)^{-1} \boldsymbol{H}^{\mathrm{H}} \boldsymbol{h}_k^{(\mathrm{tx})}} - 1. \quad (4)$$

The interpretation of (3)-(4) is that the multi-user interference at the output of the MUD is approximated as a Gaussian variate, which validity has been shown in [12]. We now face a classical decoding problem, namely *a posteriori* probability (APP) decoding of a convolutional code in additive white Gaussian noise. Since low-memory convolutional codes will be used subsequently, optimum decoding is feasible and we have deployed the log-domain BCJR algorithm [13].

### C. Channel Estimation

Assuming that the maximum normalized delay spread ($\eta_{\max}^{(\mathrm{d})}$) is within the cyclic prefix, and the channel to be static over a code block, the receiver implements a low-complexity estimator using a discrete prolate spheroidal basis representation [14] of the channel. Using the proposed model, an MMSE channel estimator is derived that uses both known pilot symbols, as well as soft data symbols based on *a posteriori* information from the SISO decoders. We omit a detailed presentation of the estimator here, and instead refer to [11] replacing Doppler domain with delay domain.

## III. EXIT Chart Representation

In order to produce an EXIT chart, information transfer functions of the different decoding blocks have to be produced. Each component decoder is viewed as a statistical Log-Likelihood-Ratio (LLR) transformer; it takes an LLR-sequence as input and outputs another (hopefully improved) version. The transfer function measures the improvement of the LLR-transformation in terms of mutual information between the LLR's and the variables that the LLR's represent. To be more specific, assume that a component decoder produces extrinsic LLR's $\Lambda_{\mathrm{ext}}$ on variables $X$ given *a priori* information $\Lambda_{\mathrm{a}}$ and possibly a set of observations. The quality of the *a priori* information is, in terms of mutual information, measured by $I_{\mathrm{a}} = I(X; \Lambda_{\mathrm{a}})$ while the quality of the output is $I_{\mathrm{ext}} = I(X; \Lambda_{\mathrm{ext}})$. The transfer function can now be statistically established as [15]

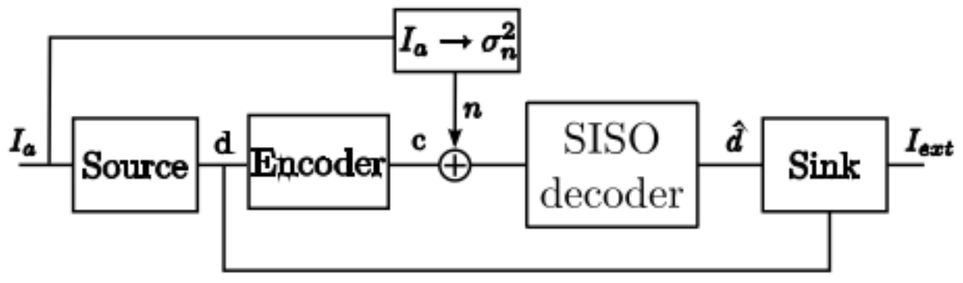


Fig. 3. System setup for producing EXIT chart for the SISO decoder.

$$I_{\mathrm{ext}} = T(I_{\mathrm{a}}). \quad (5)$$

When producing the transfer functions, all elements of $\Lambda_{\mathrm{ext}}$ (becoming $\Lambda_{\mathrm{a}}$ for the next component decoder) for both users are assumed independent and to follow a Gaussian distribution, $\mathcal{N}\left(x\mu_{\mathrm{ext}}, \sigma_{\mathrm{ext}}^2\right)$, with consistency condition $\mu_{\mathrm{ext}} = \sigma_{\mathrm{ext}}^2/2$ and where $x = \pm 1$ is the transmitted symbol. With the above given distribution of the LLR's, there is a one-to-one mapping between the mutual information $I_{\mathrm{ext}}$ and the variance $\sigma_{\mathrm{ext}}^2$ which is given by the J-function defined in [1]

$$I_{\mathrm{ext}} = J(\sigma_{\mathrm{ext}}). \quad (6)$$

The J-function is useful when generating sequences with different *a priori* information content, which is needed when generating transfer functions. In the following sections, we describe the procedure for generating transfer functions for the SISO decoder and the MUD/CE.

### A. SISO Decoder

The framework for computing the SISO EXIT curve in this paper differs from the standard approach due to the assumed channel model at the front-end of the SISO decoder ((3)-(4)), though the principles and outcome are the same. We provide a brief summary in section.

The system setup used for generating the SISO decoder transfer function is given in Fig. 3. First a number of data symbols $d$ are generated, coded with the convolutional encoder and mapped to binary symbols $c \in \{-1, 1\}$. Zero-mean Gaussian noise with variance $\sigma_{\mathrm{n}}^2$ is added to the symbols to produce the signal, $y = c + n$, feed into the SISO decoder. The variance $\sigma_{\mathrm{n}}^2$ is chosen to match a given input mutual information value $I_{\mathrm{a}}$, and some manipulations give that

$$\sigma_{\mathrm{n}}^2 = \left( \frac{2}{J^{-1}(I_{\mathrm{a}})} \right)^2.$$

After the SISO decoder the soft extrinsic output symbols are feed to the sink where the mutual information is computed through [15]

$$I_{\mathrm{ext}} = \frac{1}{2} \sum_{d=\pm 1} \int_{-\infty}^{\infty} p(\hat{d}|d) \log_2 \left( \frac{2p(\hat{d}|d)}{p(\hat{d}|-1) + p(\hat{d}|1)} \right) \partial \hat{d}, \quad (7)$$

where the probability density function, $p(\hat{d}|d)$, is approximated using histogram calculations, and the integral thus becoming a summation.

The procedure is repeated for a number of evenly spaced values of $I_{\mathrm{a}} \in ]0,1]$.

### B. MUD/CE

For the MUD/CE, the system model used for obtaining the information transfer function is shown in Fig. 4. Since the system under investigation has multiple inputs and outputs, a generalized multi-dimensional transfer function must be used. The transfer function is dependent on the channel realizations and the noise variance of the system, apart from the input a priori mutual information, and is for $K = 2$ given by

$$\left[I_{\mathrm{ext}}^{(1)}, I_{\mathrm{ext}}^{(2)}\right] = T_e\left(I_a^{(1)}, I_a^{(2)}, \boldsymbol{H}, \sigma_w^2\right) \tag{8}$$

assuming equal noise variance at both antennas.

We will shortly show that the EXIT chart depends on the specific code being used, since the input to the channel estimator is the *a posteriori* output symbols of the SISO decoder. This is a major difference compared to conventional EXIT charts. Consequently, the problem of finding suitable codes to a certain modulation scheme is no longer a "curve-matching" problem since the outer code impacts *both* EXIT curves. Note that this problem is solely a consequence of the considered MUD/CE design and not of the multi-dimensional EXIT chart technique itself. To overcome this problem we propose a modification to the MUD/CE and evaluate the impact on performance.

The transfer function is obtained in the following way. First two sets of code and pilot symbols are generated, one per user. These are then mapped to QPSK symbols, OFDM modulated, and sent through the channel. Then, given the pair of input information values, $(I_{\mathrm{a}}^{(1)}, I_{\mathrm{a}}^{(2)})$, *extrinsic* and *a posteriori* based LLR's are generated for each of the code symbols, mapped to soft QPSK symbols ($\tanh(\Lambda_x/2)$ followed by a QPSK mapper) before being sent to the MUD and CE, respectively. The LLR's are obtained as described above making use of the J-function.

Let $\Lambda_{\mathrm{ext,c}}$ and $\Lambda_{\mathrm{app,c}}$ in Fig. 4 and in the text below refer to the LLR's at the output of the decoder. To generate a sequence of input *extrinsic* based LLR's, given the input information values, is straightforward. However, the same does not hold for the corresponding *a posteriori* based LLR's $\Lambda_{\mathrm{app,c}}$ (fed to the CE). Instead, the EXIT function calculated for the SISO decoder has to be used. Assuming some *a priori* information $I_{\mathrm{a}}$, $\Lambda_{\mathrm{app,c}}$ are related to $\Lambda_{\mathrm{ext,c}}$ through

$$\Lambda_{\mathrm{app,c}} = \Lambda_{\mathrm{ext,c}} + \Lambda_{\mathrm{a,c}}, \tag{9}$$

where $\Lambda_{\mathrm{ext,c}}$ and $\Lambda_{\mathrm{a,c}}$ are independent by the definition of extrinsic information (under the assumption of large interleaver length) and $\Lambda_{\mathrm{a,c}}$ is the input LLR's to the SISO decoder. Since we are assuming an information content $I_{\mathrm{a}}$ in $\Lambda_{\mathrm{ext,c}}$, we know that $\Lambda_{\mathrm{ext,c}}$ must have been produced from $\Lambda_{\mathrm{a,c}}$ with an information content $T_c^{-1}(I_{\mathrm{a}})$. Thus, again making use of the J-function, $\Lambda_{\mathrm{a,c}}$ can be generated independently from $\Lambda_{\mathrm{ext,c}}$.

In order to simplify the evaluation of the receiver, we propose a modification that decouples the SISO decoder from the MUD/CE. By simply replacing $\Lambda_{\mathrm{app,c}}$ by $\Lambda_{\mathrm{ext,c}}$ in the feedback loop to the CE, the generated *a priori* information input, used for obtaining the EXIT surfaces, may be generated independently from the code/decoder being used. We will demonstrate that this has a minimal impact on the EXIT surface of the MUD/CE.

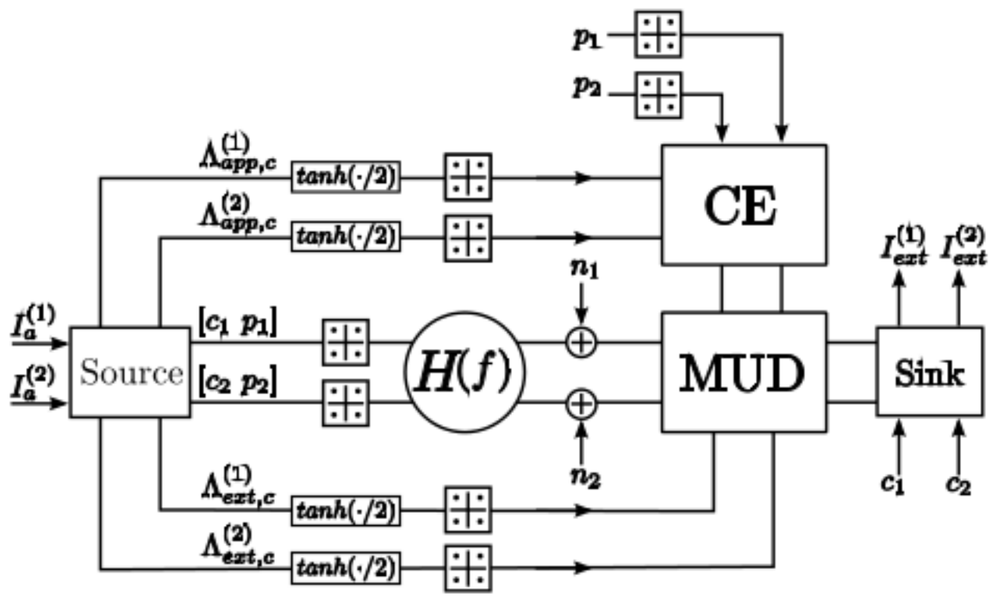


Fig. 4. System setup for producing EXIT charts for the receiver structure.

## IV. Results

The system under consideration consists of two users with one antenna each transmitting independent codewords, interleaved over time and frequency, over a frequency fading channel to a receiver having two antennas. The codewords span $S$ OFDM symbols including $S_p$ OFDM pilot symbols, where each OFDM symbol contains $M = 64$ subcarriers (see Fig. 2). Code bits are generated using a rate $1/2$ recursive systematic convolutional encoder [16] with generators $(7,5)_8$ and with two tail bits forcing the encoder to terminate in the all-zero state. A tapped delay line model with an exponential power delay profile is used to generate the channel coefficients [17], where the different transmit-receive links are generated independently of each other. Each impulse response consist of $N_{MPC} = 100$ randomly arriving multi-path components, and the normalized delay spread of the channel is set to $\eta_{\max}^{(\mathrm{d})} = 0.15$. The coherence time of the channel is assumed to be much larger than the duration of a code block; thus no variations in time are considered. Noise is added at the receiver to obtain $E_{\mathrm{b}}/N_0 = 7dB$, where $E_{\mathrm{b}}$ denotes the average total available energy per bit at the receiver and $N_0 = \sigma_w^2$.

EXIT surfaces are generated, using the above settings, for both the SISO decoder and the MUD/CE for a particular channel realization. In Fig. 6 and Fig. 7 the EXIT charts are shown, corresponding to the two different user streams, with $S = 100$ and $S_p = 1$. The upper surfaces of the figures correspond to the MUD/CE, and the lower s-shaped surfaces correspond to the SISO decoder.

When generating the EXIT surfaces for the CE/MUD shown in Fig. 6 and Fig. 7, extrinsic, instead of a posteriori, information are used as input to the CE. In Fig. 5 the diagonal of an EXIT surface for one user is shown for both the case of *extrinsic* (dashed line), and *a posteriori* (solid line), input. Clearly the discrepancy between the two is insignificant,

motivating the use of *extrinsic* information in the CE when creating EXIT surfaces for the considered receiver.

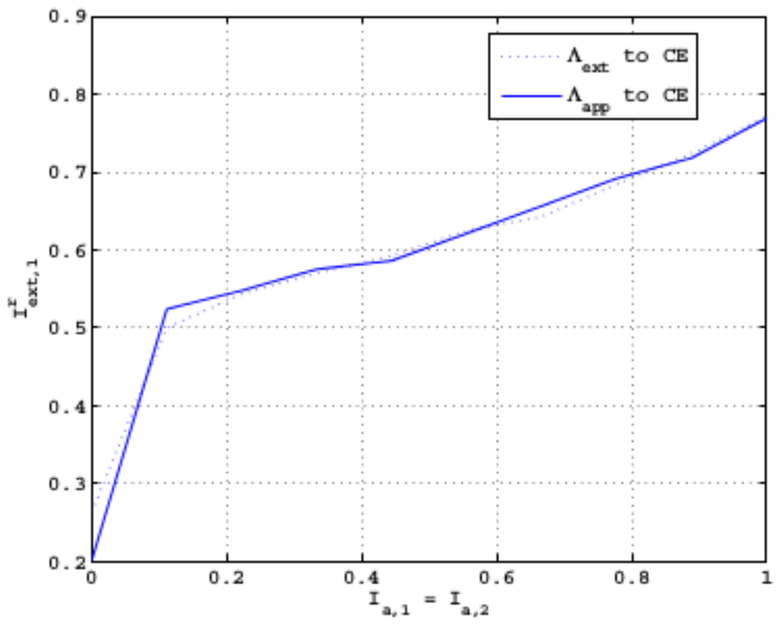


Fig. 5. Diagonal values of an EXIT surface for the CE/MUD for when extrinsic and a posteriori information is used in CE.

Moreover, since the SISO decoders are working in parallel independent of each other, the performance of one user is independent of the information content of the other, as clearly seen in Fig. 6 and Fig. 7. Looking at the surfaces corresponding to the MUD/CE; when the mutual information is zero, meaning that there is no soft information available, the output is produced without interference cancellation and only based on the initial channel estimates obtained from the pilot symbols. The starting point of the convergence path is thus dependent of the quality of the initial estimate, closely dependent on the amount of available pilot symbols. As the input information grows, Fig. 6 show that the performance of user 1 is mainly a function of the information content of the other user, with the reversed valid for user 2. This is because the accuracy of the interference cancellation is only dependent on the amount of knowledge about the interfering user. If varying the SNR, the EXIT surfaces of the MUD/CE are shifted up or down, essentially with a preserved shape. These results are not shown here.

The two paths included in the two figures show an actual decoding trajectory (solid line) and the EXIT chart prediction (dashed). The two trajectories show some differences, but they converge to the same point. For the first few iterations, there is a gap between the trajectory obtained by simulations and the surface of the MUD/CE. This discrepancy is most likely due to the mismatch between the statistics used for the LLR's, when deriving the the chart and the ones obtained from the simulations. The true LLR's show a non-Gaussian behavior, with a large variance, the first few iterations. With iterations the output LLR's become more and more Gaussian, and the gap between the chart and the decoding trajectory decrease.

In Fig. 8 the convergence area of the receiver is plotted as obtained from the EXIT charts. The area is given by

$$\left(T_{c,1}^{-1}(I_a^{(1)}, I_a^{(2)}) < T_{e,1}(I_a^{(1)}, I_a^{(2)})\right) \cup \left(T_{c,2}^{-1}(I_a^{(1)}, I_a^{(2)}) < T_{e,2}(I_a^{(1)}, I_a^{(2)})\right)$$

where the numbers in $T_{\cdot,1}$ and $T_{\cdot,2}$ refer to the separated per user transfer functions. The figure also shows the decoding trajectory and the EXIT chart prediction (with the paths of the two users superimposed on each other). As seen, the two paths follow roughly the same track, though the one obtained from simulations is lagging behind in terms of iterations. It is also worth pointing out that the point of convergence is the intersection of the four 3D surfaces. The similarities between the two trajectories changes depending on the channel realization, the block length and SNR. Our experience is that larger block lengths and higher SNR improve the fit. As a final result, we present an analysis of the impact of the multi-user channel on the performance of the receiver algorithm. We look at the EXIT curve of the MUD/CE in two points; in the initial stage when no soft information is available from the SISO decoders ($T_e(0,0)$) and when perfect knowledge about

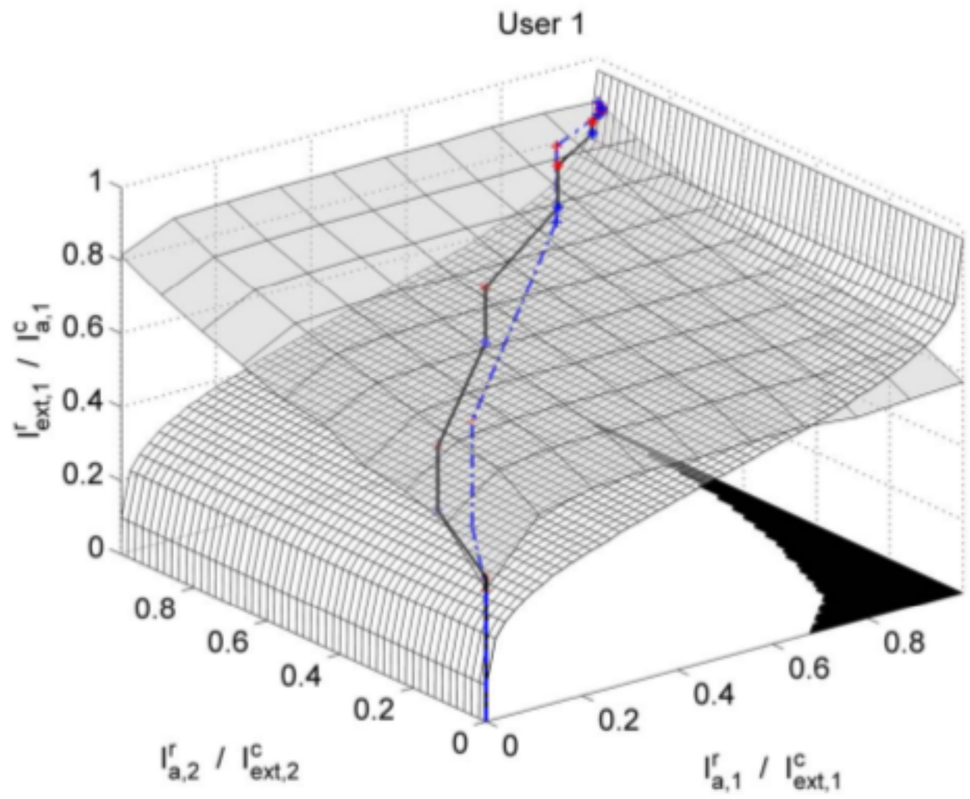


Fig. 6. EXIT chart for user 1. The solid line show an actual decoding trajectory and the dashed line the EXIT chart prediction.

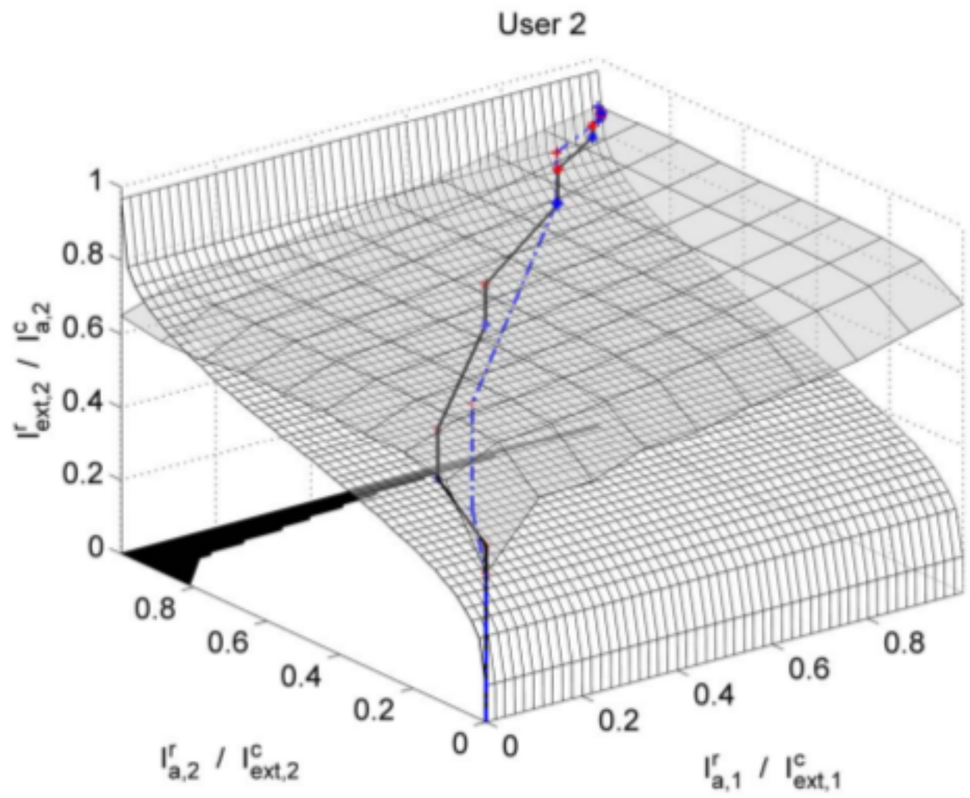


Fig. 7. EXIT chart for user 2. The solid line show an actual decoding trajectory and the dashed line the EXIT chart prediction.

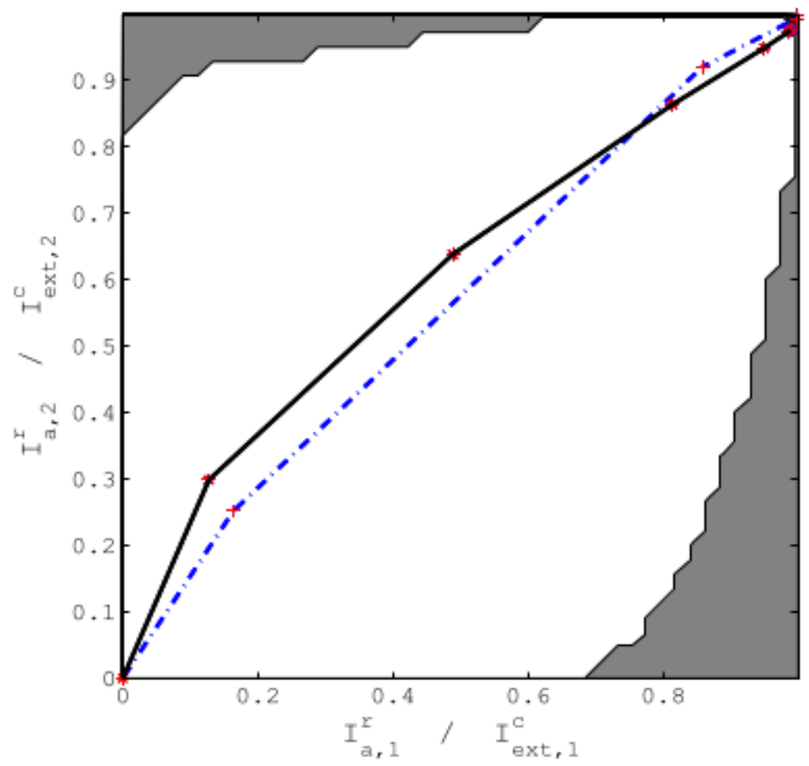


Fig. 8. Convergence area for the receiver. The figure also show the decoding trajectory and the EXIT chart prediction (with the paths of the two users superimposed on each other).

the transmitted symbols are available ($T_e(1,1)$). Fig. 9 shows the cumulative distribution functions (CDFs) of the extrinsic information output of the MUD for one of the users at an SNR ($E_b/N_0$) of 0 and 5dB, for the two cases considered. The CDFs are computed over 200 channel realizations, for the case of $S = 40$ and $S_p = 1$. The total multi-user channel power is constant over the different channel realizations. As is seen the information output show large variation depending on the quality of the channel. Though the total channel gain is constant, it will be distributed unevenly between the two users, depending on the outcome of the channel realization. Unless this is combated using an appropriate power control, the outage probability of the system will be large. If looking at the curves corresponding to the starting point ($T_e(0,0)$) we see that with an increasing SNR the quality of the initial channel estimate improve, at the same time as the number of noise induced errors decreases; thus providing a better starting point for the iterative process.

## V. Conclusions

In this paper we have studied a promising receiver candidate for non-coherent multi-antenna OFDM systems. For the considered multi-user receiver we have seen that the convergence path, and the point of convergence, can be estimated using multi-dimensional EXIT charts. We have proposed a modification of the receiver structure, simplifying the generation of the transfer function of the MUD/CE; making it possible to generate the transfer function independent of the code/decoder. This greatly simplifies the work of finding a suitable outer code for the receiver; making it into a curve fitting problem. The modifications are seen to have an insignificant impact on the transfer function.

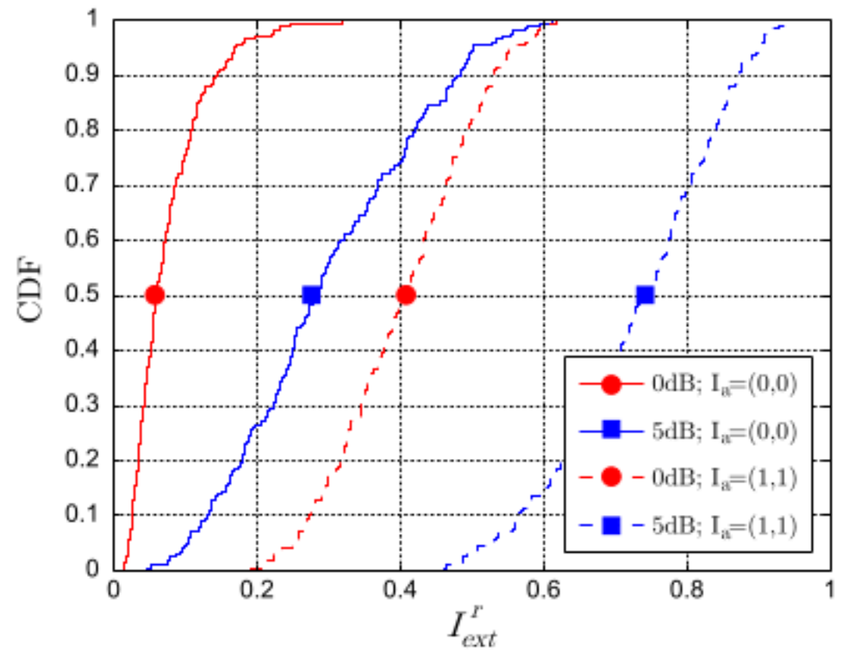


Fig. 9. The CDF of the extrinsic information output from the MUD/CE for two points, $T_e(0,0$ and $T_e(1,1)$. Results are shown for SNR values of 0 and 5dB.

## References


[1] S. ten Brink, "Convergence of iterative decoding," *Electronics Letters*, vol. 35, no. 10, pp. 806–808, May 1999.

[2] R. Koetter, A.C. Singer, and M. Tuchler, "Turbo equalization," *Signal Processing Magazine, IEEE*, vol. 21, no. 1, pp. 67–80, Jan. 2004.

[3] T. Zemen, C.F. Mecklenbrauker, J. Wehinger, and R.R. Muller, "Iterative joint time-variant channel estimation and multi-user detection for MC-CDMA," *IEEE Trans. Wireless Commun.*, vol. 5, no. 6, pp. 1469–1478, Jun. 2006.

[4] X. Wautelet, C. Herzet, A. Dejonghe, J. Louveaux, and L. Vandendorpe, "Comparison of EM-based algorithms for MIMO channel estimation," *IEEE Trans. Commun.*, vol. 55, no. 1, pp. 216–226, Jan. 2007.

[5] S. Ahmed, T. Ratnarajah, M. Sellathurai, and C. Cowan, "Iterative receivers for MIMO-OFDM and their convergence behavior," *IEEE Trans. Vehic. Tech.*, vol. 58, no. 1, pp. 461–468, Jan. 2009.

[6] K. Kansanen, *Wireless broadband single-carrier systems with MMSE turbo equalization receivers*, Ph.D. thesis, Oulu Univerity, Oulu, Finland, Dec. 2005.

[7] S. Sand, "Iterative OFDM receiver with channel estimation," in *WPMC*, San Diego, USA, Sept. 2006.

[8] D.P. Shepherd, Z. Shi, M. Anderson, and M.C. Reed, "Exit chart analysis of an iterative receiver with channel estimation," *IEEE GLOBECOM*, pp. 4010–4014, Nov. 2007.

[9] P. Salvo Rossi, P. Hammarberg, F. Tufvesson, O. Edfors, P. Almers, V.-M. Kolmonen, J. Koivunen, K. Haneda, and R.R. Muller, "Performance of an iterative multi-user receiver for MIMO-OFDM systems in a real indoor scenario," *IEEE GLOBECOM*, pp. 1–5, Nov. 2008.

[10] C. Heegard and S. B. Wicker, *Turbo Coding*, Kluwer Academic Publishers, 1999.

[11] P. Salvo Rossi and R.R. Muller, "Joint iterative time-variant channel estimation and multi-user detectionfor MIMO-OFDM systems," *IEEE GLOBECOM*, pp. 4263–4268, Nov. 2007.

[12] X Wang and H.V. Poor, "Iterative (turbo) soft interference cancellation and decoding for coded cdma," *Communications, IEEE Transactions on*, vol. 47, no. 7, pp. 1046–1061, 1999.

[13] P. Robertson, E. Villebrun, and P. Hoeher, "A comparison of optimal and sub-optimal map decoding algorithms operating in the log domain," *IEEE ICC*, vol. 2, pp. 1009–1013 vol.2, Jun. 1995.

[14] D. Slepian, "Prolate spheroidal wave functions, Fourier analysis, and uncertainty - V: The discrete case," *Bell System Technical Journal*, vol. 57, no. 5, pp. 1371–1430, May/Jun. 1978.

[15] S. ten Brink, "Convergence behavior of iteratively decoded parallel concatenated codes," *IEEE Trans. Commun.*, vol. 49, no. 10, pp. 1727–1737, Oct. 2001.

[16] J. G. Proakis, *Digital Communication*, McGraw-Hill Publishing Company, UK, fourth edition, 2000.

[17] P. Hoeher, "A statistical discrete-time model for the WSSUS multipath channel," *IEEE Trans. Vehic. Tech.*, vol. 41, no. 4, pp. 461–468, Nov. 1992.